BIOMOLECULES & THERAPEUTICS

**Original Article**
*Biomol Ther 25(4), 441-451 (2017)*

# Imperatorin is Transported through Blood-Brain Barrier by Carrier-Mediated Transporters

**Temdara Tun[1] and Young-Sook Kang[1,*]**

*[1]College of Pharmacy, Drug Information Research Institute and Research Center for Cell Fate Control, Sookmyung Women's University, Seoul 04310, Republic of Korea*

## Abstract

Imperatorin, a major bioactive furanocoumarin with multifunctions, can be used for treating neurodegenerative diseases. In this study, we investigated the characteristics of imperatorin transport in the brain. Experiments of the present study were designed to study imperatorin transport across the blood-brain barrier both *in vivo* and *in vitro*. *In vivo* study was performed in rats using single intravenous injection and *in situ* carotid artery perfusion technique. Conditionally immortalized rat brain capillary endothelial cells were as an *in vitro* model of blood-brain barrier to examine the transport mechanism of imperatorin. Brain distribution volume of imperatorin was about 6 fold greater than that of sucrose, suggesting that the transport of imperatorin was through the blood-brain barrier in physiological state. Both *in vivo* and *in vitro* imperatorin transport studies demonstrated that imperatorin could be transported in a concentration-dependent manner with high affinity. Imperatorin uptake was dependent on proton gradient in an opposite direction. It was significantly reduced by pretreatment with sodium azide. However, its uptake was not inhibited by replacing extracellular sodium with potassium or *N*-methylglucamine. The uptake of imperatorin was inhibited by various cationic compounds, but not inhibited by TEA, choline and organic anion substances. Transfection of plasma membrane monoamine transporter, organic cation transporter 2 and organic cation/carnitine transporter 2/1 siRNA failed to alter imperatorin transport in brain capillary endothelial cells. Especially, tramadol, clonidine and pyrilamine inhibited the uptake of [$^3$H]imperatorin competitively. Therefore, imperatorin is actively transported from blood to brain across the blood-brain barrier by passive and carrier-mediated transporter.

**Key Words:** Imperatorin, Alzheimer's disease, Blood-brain barrier, Proton coupled antiporter

## INTRODUCTION

Imperatorin is isolated from the root of *Angelica dahurica*. It is a major bioactive furanocoumarin (Baek *et al*., 2000). It has long been recognized that imperaotrin exhibits many biological properties such as anticancer (Kozioł and Skalicka-Woźniak, 2016), antibacterial (Stavri and Gibbons, 2005) anti-inflammatory (Abad *et al*., 2001) and HIV replication-inhibiting activities (Sancho *et al*., 2004). It is also therapeutically helpful for disorders with high anxiety level and memory impairment (Budzynska *et al*., 2012).

Alzheimer's disease (AD) and Parkinson's disease (PD) are neurodegenerative diseases characterized by cholinergic dysfunction with cholinergic deficiency in the brain (Kozioł and Skalicka-Woźniak, 2016). Imperatorin as an inhibitor of acetylcholinesterase (AChE) might be useful for treating AD and PD (Kim *et al*., 2002; Sigurdsson and Gudbjarnason, 2007). It has a small molecular weight (270 g/mol) and a large value of log P (3.65). Recently, it has been reported that imperatorin is highly passed through the blood-brain barrier (BBB) according to *in vivo* (oral administration) and *in vitro* permeability data using LC-MS/MS analysis method (Lili *et al*., 2013). However, the characteristics of imperatorin transport through the BBB remains unknown. Thus, it is important to investigate the transport characteristics of imperatorin to predict the effect of imperatorin on AD and PD.

BBB is formed by three cellular elements (astrocytes, pericytes and endothelial cells) at the lining of the tight junction. It expresses multiple transporters, which can influence the BBB permeability of their substrates (Ohtsuki and Terasaki, 2007). These transporters can mediate the blood-to-brain influx for nutrient and other essential molecules as well as the

**Open Access** **https://doi.org/10.4062/biomolther.2017.082**



**Received** Apr 4, 2017 **Revised** Apr 12, 2017 **Accepted** Apr 13, 2017
**Published Online** May 30, 2017

***Corresponding Author**
E-mail: yskang@sookmyung.ac.kr
Tel: +82-2-710-9562, Fax: +82-2-2077-7975

brain-to-blood efflux to eliminate metabolites and neurotoxic compounds from brain (Ohtsuki and Terasaki, 2007). Several influx and efflux drug transporter are expressed at the BBB, including sodium-independent glucose transporter (GLUT1/Slc2a1), monocarboxylate transporter 1 (MCT1/Slc16a1), amino acid transporter, organic anion transporter 3 (Oat3/Slc22a8), organic anion-transporting polypeptides (Oatps/Slco) and multidrug resistance-associated protein (Mrps/ ABCC) (Ohtsuki and Terasaki, 2007). Organic cation transporters (Oct1-3/Slc22a1-3), high-affinity choline transporter (ChT/Slc5a7), organic cation/carinitine transporters 1-2 (Octn1-2/Slc22a4-5), plasma membrane monoamine transporter (Pmat/Slc29a4), and multidrug and toxin extrusion protein (Mate/Slc47a) are involved in the influx and efflux transport of various cationic drugs (Okura *et al*., 2008; Roth *et al*., 2012). Organic cation drugs and opioids such as pyrilamine (Okura *et al*., 2008), oxycodone (Okura *et al*., 2008), diphenhydramine (Sadiq *et al*., 2011), tramadol (Kitamura *et al*., 2014), nicotine (Cisternino *et al*., 2013) and clonidine (André *et al*., 2009) are transported by the proton coupled antiporter. However, the molecular nature of this antiporter remains unknown. It has been reported that this transporter is dependent on energy and oppositely directed proton gradient. However, it is independent on membrane potential or sodium (Shimomura *et al*., 2013).

The objective of the present study was to investigate the transport mechanism of imperatorin across the BBB using *in vivo* intravenous injection (IV) and *in situ* internal carotid artery perfusion (ICAP) techniques. To clarify the functional properties of imperatorin influx at the BBB and its interaction with several transporters of substrates, *in vitro* uptake studies, Real-Time PCR and siRNA transfection were performed using conditionally immortalized rat brain capillary endothelial cells (TR-BBB cells).

## MATERIALS AND METHODS

### Radioisotope and reagents

Radiolabeled compound [$^3$H]imperatorin (3.7 Ci/mmol) was purchased from American Radiolabeled Chemical, Inc (St. Louis, MO, USA). Unlabeled compounds such as imperatorin, tramadol hydrochloride, pyrilamine maleate salt, verapamil hydrochloride, quinidine, nicotine, clonidine hydrochloride, 1-Methyl-4-phenylpyridinium ion ($MPP^+$) and other compounds were purchased from Sigma Aldrich (St. Louis, MO, USA).

### Animals

Male Sprague-Dawley rats (SD rats, 7 weeks, 250-350 g) were purchased from Koatech Inc (Pyeongtaek, Korea). All animal experiments were approved by the Committee of the Ethics of Animal Experimentation of Sookmyung Women's University (Seoul, Korea; Approval No.: SMWU-IACUC-16017-014).

### *In vivo* brain uptake study

**Intravenous injection technique (Pharmacokinetic):** Pharmacokinetic parameters and brain uptake of [$^3$H]imperatorin were investigated in rats following a single IV injections according to previous reports (Pardridge *et al*., 1994; Lee *et al*., 2014). SD rats were anesthetized ketamine/xylazine (100 mg/kg and 2 mg/kg; Yuhan, Seoul, Korea). [$^3$H]Imperatorin (1.35 μM) was injected to the left femoral vein of SD rat. Following administration, blood samples (0.3 mL) were collected via polyethylene 50 (PE 50) tube implanted in the left femoral artery at 0.25-60 min. At 60 min after injection, brain and other organs were collected. Organ samples were solubilized with solunene-350 (PerkinElmer, Waltham, MA, USA) and radioactivity was counted by using a Tri-Carb liquid scintillation counter (Tri-Carb 2810TR; PerkinElmer) with ultima gold (PerkinElmer).

Plasma radioactivity (dpm/ml) was converted to the percentage of injected dose (ID) per milliliter (ml). The %ID/ml was fit to a bi-exponential equation (1):

$$\%\mathrm{ID/ml} = A_1 e^{-k_1 t} + A_2 e^{-k_2 t} \quad (1)$$

The intercepts ($A_1$ and $A_2$) and the slopes ($k_1$ and $k_2$) were used to compute the pharmacokinetic parameters.

Pharmacokinetic parameters were computed as described previously (Lee *et al*., 2014) to obtain the area under the plasma concentration curve (AUC) at 60 min.

The BBB permeability-surface area (PS) product or organ clearance (μl/min/g) was determined using the following equation (2):

$$\text{PS product} = \frac{[V_D - V_0]C_p(\mathrm{t})}{\int_0^t C_p(t)dt}\ ,\ AUC\ (t) = \int_0^t C_p\ (t)dt \quad (2)$$

where $V_D$ is the terminal brain/plasma ratio or the brain volume of distribution, and $V_0$ is the plasma volumes for the respective organs and $C_p$ (t) is the terminal plasma concentration (%ID/ml). The terminal brain uptake, expressed as %ID/g brain, was calculated from the PS (μl/min/g) and the 60-min plasma AUC (%ID min/ml) using the following equation (3):

$$\%\mathrm{ID/g\ (t)} = \text{PS product} \times \mathrm{AUC\ (t)} \quad (3)$$

**Brain uptake index method (BUI):** BUI technique was performed as reported previously (Suzuki *et al*., 2002). After rat was anesthetized with ketamine, the common carotid artery was injected with 200 μl Ringer-HEPES buffer containing [$^3$H]imperatorin (2.5 μCi) with or without unlabeled inhibitor compound and [$^{14}$C]*n*-butanol (0.5 μCi) used as an internal reference compound. Rat was decapitated 15 s after injection and cerebrum were dissolved in solunene-350. Their radioactivity was performed using Tri-Carb Liquid Scintillation Counters. The distribution characteristic of [$^3$H]imperatorin were expressed using the percentage of [$^3$H]imperatorin uptake relative to [$^{14}$C]*n*-butanol that was expressed by Eq (4):

$$\mathrm{BUI\ (\%)} = \frac{\left\{\frac{[3\mathrm{H}]}{[14\mathrm{C}]}(\text{dpm in the brain})\right\}}{\left\{\frac{[3\mathrm{H}]}{[14\mathrm{C}]}(\text{dpm in the injectate solution})\right\}}\ \mathrm{X}\ 100 \quad (4)$$

**Internal carotid artery perfusion technique:** ICAP technique was performed as reported previously (Takasato *et al*., 1984; Lee and Kang, 2016). SD rats were anesthetized with ketamine/xylazine (100 mg/kg and 2 mg/kg). [$^3$H]Imperatorin (270 nM) with or without unlabeled imperatorin and inhibitor compounds were diluted in KHB and perfused into the internal carotid artery of rat at a flow rate of 4mL/min for 15 sec using micro-syringe pump. To examine [$^3$H]imperatorin transport on pH alteration, HCl or NaOH was added to KHB in some experiments after gassing to bring the pH to 6.40, 7.40 or 8.40.

The ionic composition of the KHB perfusate was changed by 256 mM of mannitol instead of $Na^+$ and $Cl^-$. Rat was also perfused with carbonate-free HEPES-buffered saline.

$V_D$ of the [$^3$H]imperatorin was determined from the ratio activity of disintegrations per minute per gram (dpm/g) of brain.

$$V_D(\mu\ell/g) = \frac{[\text{brain(dpm)/brain(g)}]}{[\text{perfusate(dpm)/perfusate}(\mu\ell)]}$$

The BBB permeability surface area (PS) product was calculated using the following equation (5):

$$PS(\mu\ell/\text{min/g}) = V_D(\mu\ell/g)/\,t\ \textit{(min)} \quad (5)$$

where $V_D$ was the brain volume of the [$^3$H] compound and t was the perfusion time (15 Sec).

For the concentration-dependency experiment (André *et al*., 2009), the flux of [$^3$H]imperatorin was calculated from the flux ($J_{in}$; nmol/min/g of brain) is given by equation (6):

$$J_{in} = PS \times C_{tot} \quad (6)$$

The [$^3$H]imperatorin brain flux (Jin) or cellular velocity (μmol/min/g) was described as saturable (Michaelis-Menten term). A passive unsaturable component has been measured with equation (7):

$$J_{in} = \frac{V_{max}\ C_{tot}}{K_m + C_{tot}} + K_{passive}\ C_{tot} \quad (7)$$

where $C_{tot}$ (mM) was the total imperatorin concentration in perfusate or incubation buffer, $V_{max}$ (μmol/min/g) is the maximal velocity of transport, and $K_m$ (mM) of imperatorin was the concentration at the haft-maximal carrier velocity. $K_{passive}$ (μL/min/g) was an unsaturable component representing the rate transport by passive diffusion. Data were fitted using nonlinear regression analysis.

**[$^3$H]Imperatorin uptake study in TR-BBB cells:** TR-BBB cells were cultured according to a previously report (Terasaki and Hosoya, 2001; Kang *et al*., 2002). For *in vitro* uptake study, [$^3$H]imperatorin transport in TR-BBB cells was performed described previously (Kang *et al*., 2002). Cells were then incubated with 200 μL transport buffer containing 135 nM [$^3$H]imperatorin with or without selected compounds at 37°C for a designed time. Aliquots were collected to count the radioactivity using the Tri-Carb Liquid Scintillation Counter. Cellular protein content was determined with a DC protein assay kit using bovine serum albumin (Bio-Rad Laboratories Co, Hercules, CA, USA) as a standard. [$^3$H]Imperatorin uptake was expressed as cell-to-medium (μL/mg protein) ratio as follows: radioactivity (dpm/μL) in the sample per milligram cell protein (dpm/mg protein).

The initial uptake of imperatorin was measured for 5 min For kinetic studies, the Michaelis-Menten constant ($K_m$) and the maximum uptake rate ($V_{max}$) of [$^3$H]imperatorin were estimated using the following equation (8):

$$V = V_{max} \cdot C/(K_m + C) + K_d \cdot C\ (1) \quad (8)$$

where V and C were the initial uptake rate of [$^3$H]imperatorin at 5 min and the concentration of imperatorin, respectively. $V_{max}$ was the maximum uptake rate for the saturable component, and $K_d$ was the first order constant for non-saturable component respectively.

$V_{max}/K_m$ (μL/min/mg protein) value was calculated as the uptake clearance for saturable transport compound. The saturable component of imperatorin was plotted by non saturable uptake from total uptake in Eadie-Hofstee plot.

The inhibitory constant ($K_i$) was in the presence of 1 mM tramadol, clonidine or pyrilamine. It was calculated from the following equation (9):

$$V = V_{max} \times C/[K_m \times (1 + I/K_i) + C] + K_d \times C \quad (9)$$

where I was the concentration of each mutual inhibitory effects of compound, as the inhibitor concentration.

Energy, sodium ion and membrane potential dependency of imperatorin uptake by TR-BBB cells were determined as described previously (Kitamura *et al*., 2014). The uptake was evaluated under ATP-depleted condition by 20 min pre-incubation with 0.1% of sodium azide ($NaN_3$) and 25 μM of rotenone (dissolved in the transport buffer containing 0.2% DMSO) which were metabolic energy inhibitor. In this experiment, 10 mM D-glucose in the ECF buffer was replaced by 10 mM 3-*O*-methylglucose to reduce metabolic energy. To assess sodium ion dependency, the uptake was measured under sodium ion-free conditon by replacing NaCl in ECF buffer with $NMG^+$. The uptake also performed under membrane-disrupted condition by replacing of sodium ion with KCl followed by treatment with 10 μM valinomycin (transport buffer containing 0.2% DMSO) for 10 min. In order to evaluate the effect of proton gradient on imperatorin uptake by TR-BBB cells, cells were simultaneously treated with 10 μM carbonyl cyanide-p-trifluoromethoxyphenylhydrazone (FCCP, a protonophore). FCCP was dissolved in transport buffer containing 0.10% DMSO. For extracellular pH ($pH_e$) dependent, [$^3$H]imperatorin uptake at pH 6.4 and pH 8.4. To examine the effect of intracellular pH ($pH_i$) dependent, cells were pre-treated with 30 mM of ammonium chloride ($NH_4Cl$) for 30 min to reduce $pH_i$ and simultaneously treated with 30 mM NH4Cl to increase $pH_i$ (Okura *et al*., 2008).

## RNA interference analysis

For gene silencing of a set of four siRNAs (GE Healthcare Dharmacon, Inc., Landsmeer, Netherlands) specific for rOctn2, rPmat, rOcnt1, rOct2 and negative control were used in TR-BBB cells, including target sequences of Octn2, rPmat, rOcnt1, rOct2 and negative control. TR-BBB cells were seeded onto collagen-coated 6- and 24- well plates at a density of $1\times10^5$ cells/cm$^2$. At 24 h after seeding, siRNAs specific for Octn2, Pmat, rOcnt1and rOct2 (200 nM) or negative control siRNA (control) were transfected into TR-BBB cells using Lipofectamine® 2000 transfection reagent (Invitrogen, Carlsbad, CA, USA) according to manufacturer's protocol. Cells were used for quantitative real-time PCR and [$^3$H]imperatorin uptake was analyzed at 48 h after the initiation of transfection (Lee and Kang, 2016).

## Statistical analysis

All data were expressed as means ± standard error of the means (SEM). Statistical analysis of data was performed by one-way ANOVA analysis of variance followed by Dennett's (post hoc test) for single and multiple comparisons, respectively. Statistically significant was considered at $p<0.05$.

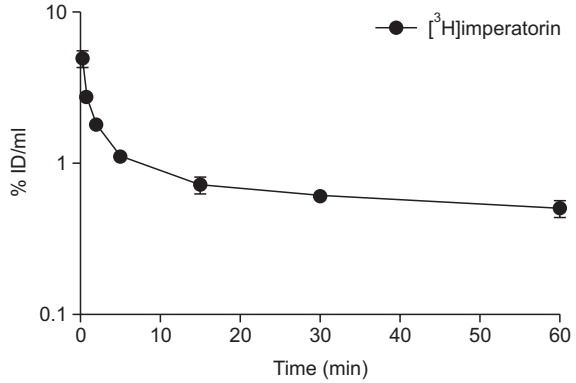


**Fig. 1.** Clearance from plasma of [$^3$H]imperatorin for up to 60 min after single intravenous injection in SD rats. Each point represents the mean ± SEM (n=3 rats).

## RESULTS

### *In vivo* brain uptake of [$^3$H]imperatorin across the blood-brain barriers

First, brain uptake and pharmacokinetic parameters of imperatorin across the BBB were examined following IV injection of [$^3$H]imperatorin in rats. Time course result of [$^3$H]imperatorin clearance from blood in SD rats was shown in Fig. 1. Pharmacokinetic parameters by analyzing data in Fig. 1 are listed in Table 1A. Plasma AUC and BBB PS products of [$^3$H]imperatorin were 22 ± 1%ID min/mL and 3.94 ± 0.54 μl/min/g, respectively (Table 1A). Thus the BBB PS product of [$^3$H]imperatorin was 12 fold higher than BBB PS product of sucrose (0.32 ± 0.52 μl/min/g) (Lee and Kang, 2016). The volume of distribution ($V_D$) of [$^3$H]imperatorin (392 ± 32 μl/g) in brain hemisphere at 60 min after IV injection was higher than $V_D$ of [$^{14}$C]sucrose (68 ± 9 μl/g) (data not shown) (Lee and Kang, 2016). The clearance of [$^3$H]imperatorin by other peripheral tissues such as heart, liver, lung and kidney is shown in Table 1B. Uptake of [$^3$H]imperatorin by the brain in rats was 0.086 ± 0.008%ID/g (Table 1B). These results indicated that imperatorin was actively taken up into the brain across the BBB under physiological condition.

In order to confirm the blood-to-brain transports mechanism, mperatorin was also measured with the ICAP technique. The brain volume distribution (corrected $V_D$) value of [$^3$H]imperatorin was 615 ± 3 μl/g after perfusion (data not shown). The $V_D$ was sixty fold greater than the $V_D$ of [$^{14}$C]sucrose, the plasma volume marker (Pardridge *et al*., 1994). Brain $V_D$ of [$^3$H]imperatorin was decreased at pH 6.4, while brain $V_D$ of [$^3$H]imperatorin was increased at pH 8.4 compared to that of the control (Fig. 2). A decrease in the $pH_i$ can lead to inversion of the proton gradient that favors the movement of the proton out of cells. The brain transport of [$^3$H]imperatorin was significantly increased in mannitol $Na^+$-free buffers compared with control (Fig. 2). However brain transport of [$^3$H]imperatorin was markedly decreased in carbonate-free HEPES. Therefore, imperatorin is actively transported from blood to the brain across the BBB. It depends on opposite direction of proton gradient.

Brain influx of imperatorin was found to be concentration dependent (Fig. 3). The used concentrations were reflected unsaturated and saturated conditions (lower than 0.25 mM, Fig. 3 insert). The plot of influx against total imperatorin concentration yielded an apparent $K_m$ of 0.18 mM and $V_{max}$ of 0.50 μmol/min/g. Unsaturated apparent component ($K_d$) certainly reflected passive diffusion. Nonlinear regression analysis gave $K_d$ of $3.1\times10^{-17}$ μL/min/g representing a very small value of total brain imperatorin influx. This suggests that involvement of influx transporter in luminal side of the BBB transport of imperatorin. Cationic drug such as tramadol, pyrilamine, clonidine and verapamil strongly inhibited [$^3$H]imperatorin uptake in rat brain based on ICAP (Table 2). The uptake of [$^3$H]imperatorin was also strongly inhibited by other cationic drug such as $MPP^+$ (Pmat substrate) (Okura *et al*., 2011), ALC, and L-carnitine (Kido *et al*., 2001). However, some cationic compounds in Table 2 such as TEA (substrate of OCTs, Octn1, and Mates) (Tamai *et al*., 2004; Ohta *et al*., 2006) and choline (ChT substrate) (Kang *et al*., 2005) did not affect [$^3$H]imperatorin transport in the brain. Moreover, [$^3$H]imperatorin uptake was not changed by organic anion such as PAH (Oat3 subtrate) (Hosoya *et al*., 2009) or 6-Mercaptopurine either (6-Mp,Oat3 and Mrps substrate) (Hosoya *et al*., 2009; Lee *et al*., 2011). In addition, the BUI value of [$^3$H]imperatorin was 50.4%. The BUI of [$^3$H]imperatorin was significantly inhibited by unlabeled imperatorin (1 mM), 10 mM of verapamil, nicotine, pyrilamine, clonidine (Table 3). However [$^3$H]imperatorin uptake was not changed by 10 mM of TEA and PAH. These results indicate that imperatorin across the BBB and *in vivo* brain uptake of its may be also involved in carrier-mediated transport system.

**Table 1.** Pharmacokinetic parameters (A) and brain volume of distribution (VD), BBB PS products, the other organs distribution (%ID/g) (B) of [$^3$H]imperatorin after single intravenous (IV) injection in SD rats

**A**

| Parameters | Imperatorin (n=3) |
|---|---|
| $T_{1/2}$ (min) | 51.9 ± 4.8 |
| AUC (% ID min/mL) | 22.1 ± 0.8 |
| AUCss (% ID min/mL) | 38.2 ± 1.5 |
| Vdss (mL/kg) | 183 ± 7 |
| CL (mL/min/kg) | 2.62 ± 0.1 |
| MRT (min) | 70.0 ± 4.4 |

**B**

| Organ | [$^3$H]imperatorin | |
|---|---|---|
| | Organ clearance (μl/min/g) | Uptake (%ID/g) |
| $V_D$ (μL/g) | | 392 ± 30 |
| Brain | 3.94 ± 0.5 | 0.086 ± 0.008 |
| Heart | 73.7 ± 5.9 | 1.62 ± 0.10 |
| Liver | 54.7 ± 2.5 | 1.21 ± 0.08 |
| Lung | 76.4 ± 3.4 | 1.68 ± 0.03 |
| Kidney | 168 ± 17 | 3.70 ± 0.33 |

Parameters computed from the plasma radioactivity profile in Fig 1. $V_D$, BBB PS products, %ID/g and pharmacokinetic parameters were estimated after IV injection of [$^3$H]imperatorin (1.35 μM) at 60 min in SD rats. Each value represents mean ± SEM (n=3). $T_{1/2}$: half-life; AUC: area under the curve of plasma concentration; CL: clearance; MRT: mean residence time; $V_{d,ss}$: plasma volume of distribution at steady state.

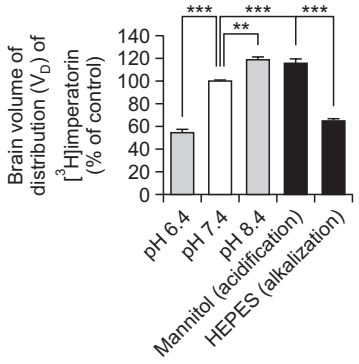


**Fig. 2.** Effects of changes in vascular perfusion fluid $pH_e$ (gray columns) and intracellular endothelial $pH_i$ (black column) on [$^3$H] imperatorin uptake in rat brain. The percentage of $V_D$ was estimated after internal carotid artery perfusion of [$^3$H]imperatorin at pH 6.4, 7.4 or 8.4. Internal carotid artery perfusion buffer was Krebs-carbonate buffer plus mannitol (sodium-free and chloride-free) and carbonate-free HEPES to alterto acidification and alkalization, respectively. Each value represents means ± SEM (n=3 SD rats). **$p$<0.01, ***$p$<0.001, significantly different from the control.

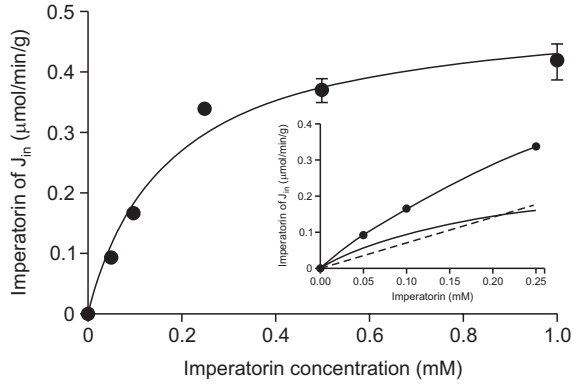


**Fig. 3.** Imperatorin brain influx ($J_{in}$, μmol/min/g) was estimated after internal carotid artery perfusion in SD rats with imperatorin concentration (0-1 mM) in the Krebs-carbonate perfusion fluid at pH 7.4. Each points represent mean ± SEM (n=3 rats). The total uptake (●) was analyzed as the sum of saturable (solid curve) and nonsaturable (dashed line) components. Data were fitted to the Michaelis-Menten equation by nonlinear least-square regression.

**Table 2.** Inhibitory effect of various compounds on [$^3$H]imperatorin brain uptake following internal carotid artery perfusion in SD rats

| Compound | Concentration (mM) | Brain volume of distribution ($V_D$, % of Control) |
|---|---|---|
| Control | | 100 ± 0 |
| Imperatorin | 1 | 17.2 ± 1.7*** |
| Tramadol | 1 | 79.2 ± 3.8*** |
| Paeonol | 1 | 56.8 ± 71.9*** |
| Verapamil | 1 | 15.1 ± 2.3*** |
| Pyrilamine | 1 | 59.2 ± 2.6*** |
| Clonidine | 1 | 69.5 ± 1.5*** |
| MPP+ | 1 | 56.3 ± 5.8*** |
| ALC | 1 | 58.1 ± 1*** |
| L-Carnitine | | 79.2 ± 5.3*** |
| TEA | 1 | 103 ± 5 |
| Choline | 1 | 99.1 ± 3.3 |
| PAH | 1 | 94.4 ± 7.1 |
| 6-MP | 1 | 102 ± 2 |

Inhibition of [$^3$H]imperatorin brain uptake by other compounds 1 mM was evaluated using internal carotid artery perfusion technique at rate of 4 ml/min for 15 sec in SD rats, pH7.4. Each value represents mean ± SEM (n=3~7). ***$p$<0.001, significantly different from the control.

**Table 3.** Brain uptake index (BUI) of [$^3$H]imperatorin

| Inhibitor | Concentration (mM) | BUI (%) |
|---|---|---|
| Control | | 50.4 ± 1.8 |
| Impeatorin | 1 | 24.9 ± 3.4*** |
| Verapamil | 10 | 22.1 ± 3.8*** |
| Nicotine | 10 | 27.6 ± 0.0*** |
| Pyrilamine | 10 | 29.1 ± 1.7*** |
| Clonidine | 10 | 33.9 ± 5.5 ** |
| TEA | 10 | 48.6 ± 4.5 |
| PAH | 10 | 58.5 ± 6.3 |

A mixture of [$^{14}$C]butanol and [$^3$H]imperatorin was injected into the common carotid artery in the presence or absence of various inhibitors. Rats were decapitated at 15 s after injection. Each value represents the mean ± SEM (n=3~6). **$p$<0.01, ***$p$<0.001; significantly different from control.

### *In vitro* characteristics of the [$^3$H]imperatorin transport mechanism by TR-BBB cells

To determine the mechanism of [$^3$H]imperatorin uptake into brain, TR-BBB cell lines were used as a rat *in vitro* model of BBB. Uptake of [$^3$H]imperatorin was time-dependent. It was increased linearly until 5 min at pH 7.4 (Fig. 4A). Therefore, uptake was evaluated at 5 min in the following kinetic and inhibition studies. The effect of $pH_e$ on imperatorin uptake by TR-BBB cells was examined by incubating ECF-buffer containing [$^3$H]imperatorin at pH 6.4, 7.4 or 8.4. [$^3$H]Imperatorin uptake was significantly reduced at pH 6.4, while it was markedly increased at pH 8.4 compared to that of the control (Fig. 5A). To confirm the result of pHe alteration, the effect of $pH_i$ alteration on [$^3$H]imperatorin uptake by TR-BBB cells was continuously examined. [$^3$H]Imperatorin uptake was reduced when $pH_i$ became alkalized that induced by 30 mM $NH_4Cl$, while was increased at intracellular acidification condition induced by 20 min pretreatment of $NH_4Cl$ (Fig. 5B). To test the driving force of [$^3$H]imperatorin uptake, pretreatment with protonophore, FCCP, was performed for 10 min. FCCP decreased [$^3$H]imperatorin uptake compared to the control (Table 4). These results suggest that the uptake of imperatorin is driven by an oppositely directed proton gradient. [$^3$H]Imperatorin uptake was also markedly reduced by pretreatment with metabolic inhibitors such as rotenone or sodium azide compared to that in the control. In contrast, uptake of imperaotrin was not significantly decreased by replacement of sodium with N-methylglucamine$^+$ or potassium chloride. Moreover, uptake of [$^3$H]imperatorin was not changed by 10 min treatment with valinomycin, a potassium ionophore (Table 4). These results indicate that imperatorin uptake through the BBB is transported by proton coupled antiporter and it is energy dependent, but

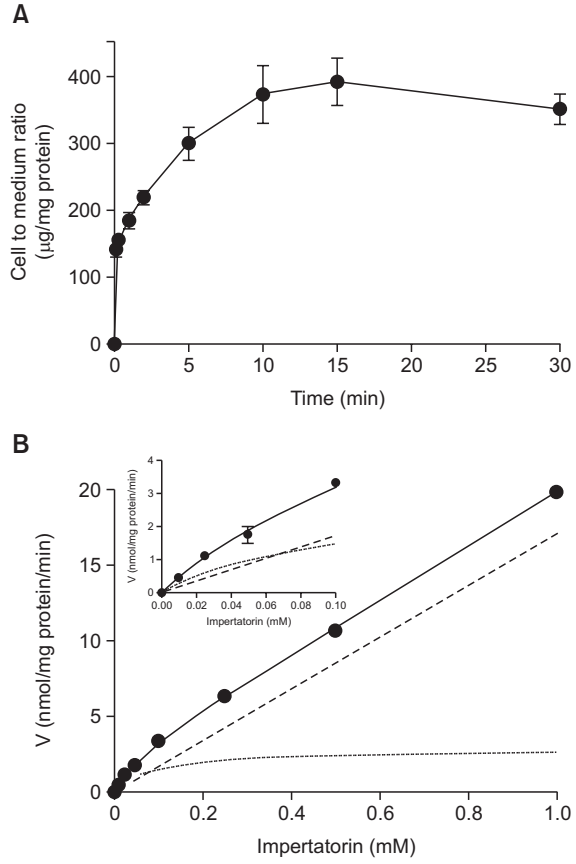


**Fig. 4.** Time courses uptake of [$^3$H]imperatorin by TR-BBB cells (A). Uptake of [$^3$H]imperatorin was measured at 37°C. Each point represents the mean ± SEM (n=3). Concentration-dependence of the initial uptake rate of [$^3$H]imperatorin uptake was measured in TR-BBB cells after with 5 min incubation with 0-1 mM unlabeled imperatorin at pH 7.4 (B). The total uptake (●) was analyzed as the sum of saturable (dashed curve) and nonsaturable (dashed line) components. Values are presented as means ± SEM (n=3).

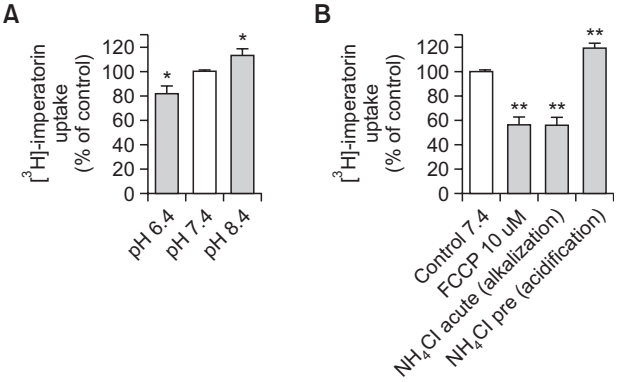


**Fig. 5.** The effect of $pH_e$ (A) and $pH_i$ (B) alteration on [$^3$H]imperatorin uptake into TR-BBB cells. [$^3$H]Imperatorin uptake was measured in buffer pH values of 6.4, 7.4, or 8.4 (B). [$^3$H]Imperatorin uptake was measured under conditions of intracellular acidification and alkalization induced by NH4Cl (B). Each column represents the mean ± SEM (n=4). **p*<0.01, ***p*<0.001, significantly different from the control.

**Table 4.** Effect of metabolic inhibitor, protonophore, sodium replacement and membrane potential disruption on [$^3$H]imperatorin uptake by TR-BBB cells

| Treatment | Relative Uptake (% of Control) |
|---|---|
| Metabolic inhibitor | |
| Sodium azide (0.1%) | 63.8 ± 2.7*** |
| Rotenone | 56.9 ± 4.4*** |
| Protonophore | |
| 10 μM FCCP | 56.2 ± 6.3** |
| Na+replacement | |
| *N*-Methylglucamine (NMG) | 97.4 ± 6.6 |
| Membrane potential | |
| 10 μM Valinomycin | 87.0 ± 2.1 |
| Potassium ion (KCl) | 97.3 ± 2.3 |

Uptake of [$^3$H]imperatorin by TR-BBB cells was performed at 37°C for 5 min in the absence or presence of a compound at pH 7.4. FCCP and valinomycin were dissolved in the transport buffer containing 0.2% ethanol and pre-incubated with cells for 10 min. These studies were performed in parallel with appropriate control containing corresponding ethanol concentration. Each value represents the mean ± SEM (n=3~4) ***p*<0.01, ****p*<0.001, significantly different from the control.

not sodium or membrane potential dependent.

To characterize the kinetics of imperatorin uptake by TR-BBB cells, [$^3$H]imperatorin uptake at various concentrations of unlabeled imperatorin (0.01~1 mM) was examined. Calculation for kinetic parameters of imperatorin revealed Michaelis-Menten constant ($K_m$) of 59 μM and a maximum rate of uptake velocity ($V_{max}$) of 2.22 nmol/mg protein/min (Fig. 4B). Nonsaturable uptake clearance ($K_d$) of imperatorin was 17 μL/(mg protein×min).

The transporter(s) responsible for imperatoirn uptake into TR-BBB cells was determined by testing the inhibitory effect of several compounds clearly related to BBB transporters. Uptake of [$^3$H]imperatorin was strongly inhibited by several cationic drugs such as tramadol, pyrilamine, diphenhydramine, clonidine, nicotine, verapamil (Kubo *et al*., 2013), and quinidine (Table 5). Organic cation, $MPP^+$, ALC, and L-carnitine moderately inhibited [$^3$H]imperatorin uptake. However some compounds as shown in Table 4, TEA, choline, PAH, estrone-3-sulfate (Oatps) (Sai *et al*., 2006) and 6-Mp failed to inhibit [$^3$H]imperatorin uptake.

*In vivo* and *in vitro* results showed that imperatorin uptake was inhibited by $MPP^+$, L-carnitine, and ALC. Therefore imperatorin uptake could be mediated by Pmat or Octn2. To evaluate whether imperatorin transport was mediated by Pmat and Octn2, siRNA transfection was performed to knockdown rPmat and rOctn2 in TR-BBB cells. Quantitative real-time PCR analysis showed that rPmat, Oct2, Octn2 and rOctn1 siRNA decreased mRNA expression levels of rPmat and Octn2 to 33.5%, 59.4%, 60.6% and 47.8%, respectively, compared to control siRNA (data not shown). Moreover, [$^3$H]$MPP^+$ and [$^3$H] ALC uptakes were significantly inhibited by rPmat and Octn2 siRNA, respectively (Fig. 6A, 6B). In contrast, [$^3$H]imperatorin uptake was not significantly affected by rPmat, rOct 2, rOctn2 or rOctn1 siRNA transfection (Fig. 6C, 6D).

The plots of [$^3$H]imperatorin uptake with or without 1 mM of tramadol, pyrilamine or clonidine intersected at the ordinate axis. These results demonstrate that tramadol, pyrilamine and

**Table 5.** Inhibitory effects of selected compounds on [$^3$H]imperatorin uptake by TR-BBB cells

| Compound | Concentration (mM) | Relative Uptake (% of Control) | Predicted Log *D* |
|---|---|---|---|
| Control | | 100 ± 3 | |
| + Imperatorin | 1 | 44.7 ± 2.6*** | 2.98 |
| + Tramadol | 1 | 71.7 ± 4.7** | 0.29 |
| + Tramadol | 10 | 35.4 ± 4.7*** | |
| + Paeonol | 1 | 46.8 ± 2.1*** | 2.3 |
| + Paeonol | 10 | 40.8 ± 1.6*** | |
| + Verapamil | 1 | 66.2 ± 8.5*** | 2.46 |
| + Pyrilamine | 1 | 65.3 ± 3.7*** | 0.76 |
| + Quinidine | 1 | 65.4 ± 2.8*** | 0.98 |
| + Clonidine | 1 | 66.2 ± 2.3*** | 1.60 |
| + Nicotine | 1 | 68.3 ± 3.7*** | -0.62 |
| + Diphenhydramine | 1 | 56.9 ± 6.7** | 3.43 |
| + MPP+ | 1 | 81.3 ± 3.9* | -0.29 |
| + ALC | 1 | 84.9 ± 1.8* | -3.43 |
| + L-Carnitine | | 86.4 ± 5.6 | -4.13 |
| +TEA | 1 | 107 ± 10 | -3.26 |
| + Choline | 1 | 100 ± 5 | -4.14 |
| + PAH | 1 | 90.3 ± 5.7 | -3.69 |
| + $E_1S$ | 1 | 103 ± 6 | -1.40 |
| +6-MP | 1 | 127 ± 9 | -3.09 |

The uptake of [$^3$H]imperatorin by TR-BBB cells was measured in the absence (control) or presence of compounds at 37°C for 5 min. Each value represents the mean ± SEM (n=3~4). *$p$<0.05, **$p$<0.01, ***$p$<0.001, significantly different from the control.

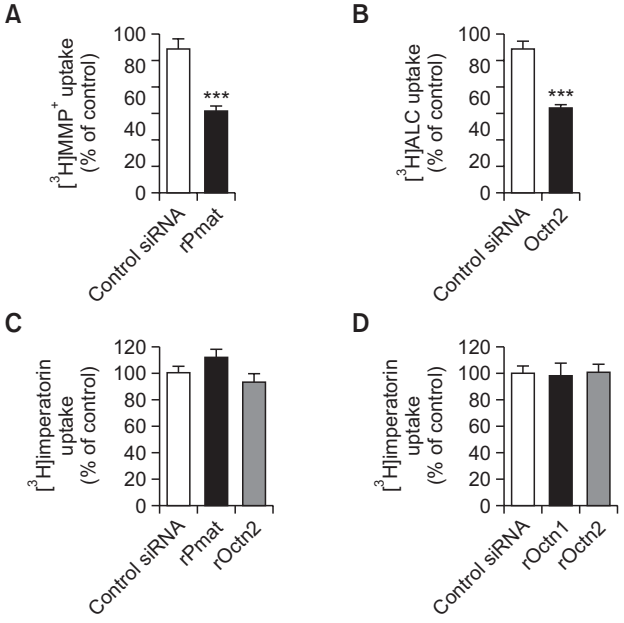


**Fig. 6.** Effect of rPmat and rOctn2 siRNA on [$^3$H]MPP$^+$(A), [$^3$H] ALC (B) and [$^3$H] imperatorin (C) uptake in TR-BBB cells. Effect of rOctn1 and rOct2 siRNA on imperatorin uptake in TR-BBB cells (D). [$^3$H]MPP$^+$, [$^3$H]ALC and [$^3$H]imperatorin uptakes were determined at 37°C for 5 min. Each column represents the mean ± SEM (n=3). ***$p$<0.001, significantly different from the siRNA control.

clonidine competitively could inhibite [$^3$H]imperatorin uptake with $K_i$ value of 16 μM, 44 μM and 1 mM, respectively (Fig. 7).

## DISCUSSION

Neurodegenerative diseases such as Alzheimer's disease (AD) and Parkinson's disease (PD), were found that deficient of Ach based on the activity studies of the acetylcholinesterase (AChE) (Kozioł and Skalicka-Woźniak, 2016). Imperatorin, a furanocoumarin derivative, has been documented to have many pharmacological properties for possible drug development. It has been examined as an AChE inhibitor with prospects of AD and PD therapy (Senol *et al*., 2011; Budzynska *et al*., 2015). However, transport mechanism of imperatorin into the brain remains unclear. In this present study, the function of imperatorin transport across the BBB was investigated using *in vivo* and *in vitro* approaches.

*In vivo* analysis, plasma pharmacokinetics of imperatorin in SD rat are shown in Table 1 and Fig. 1. Results indicated that imperatorin was eliminated rapidly. This rapid systemic clearance is principally due uptake by other organs (Table 1). BBB PS products of imperatorin was 20-fold greater than that of sucrose by IV injection in previous report (Wu and Pardridge, 1999). In addition, brain uptake of imperatorin has been reported to be the same as %ID/g of morphine (0.0810 ± 0.0005) (Wu *et al*., 1997). Following IV injection result, $V_D$ of [$^3$H]imperatorin in rat brain was nearly 6 fold higher than the $V_D$ of [$^{14}$C]sucrose, a maker for vascular space (Table 1B) (Lee and Kang, 2016). This result suggests that imperatorin might be actively transported to brain through the BBB under physiological state. Moreover, the $V_D$ of [$^3$H]imperatorin in rat brain following ICAP technique was 60 fold greater than the $V_D$ of [$^{14}$C]sucrose (Pardridge *et al*., 1994). This $V_D$ value was similar to that of 4-phenylbutyrate readily taken up by the brain through the monocarboxylate transporter 1 (MCT1) (Lee and Kang, 2016). It was also similar to that of taurine mediated by taurine transporter (TAUT) in BBB (Kang, 2000; Kang *et al*., 2002). Our results suggeste that imperatorin is actively and highly transported through the BBB to the brain.

High BBB permeability of imperatorin in mice has been reported in previous studies (Lili *et al*., 2013). However, the mechanism of imperatorin transport by brain is unknown. *In vivo* [$^3$H]imperatorin uptake was shown to be concentration dependent and saturable in this study (Fig. 3). The apparent BBB Michaelis-Menten ($K_m$) parameter for imperatorin transport in the rat brain (pHe 7.4) agreed well with the *in vivo* $K_m$ value in clonidine (proton coupled antiporter substrate) mouse using *in situ* brain perfusion (0.6 mM) (André *et al*., 2009). The unsaturated component ($K_d$) confirms that passive diffusion of imperatorin is negligible. These data suggest that imperatorin uptake by brain is regulated by specific carrier-mediated transporter with imperaotorin concentration under 250 μM. Based on *in vivo* transport mechanism study, imperatorin uptake was significantly increased at $pH_e$ 8.4 and after intracellular acidification induced by mannitol (Fig. 2). On the other hand, decreased imperatorin transport was observed at lower pHe (pH 6.4) and after intracellular alkalization induced by HEPES (Fig. 2). Similar results have been reported in previous studies (André *et al*., 2009; Sadiq *et al*., 2011; Cisternino *et al*., 2013; Chapy *et al*., 2014). These results indicate that imperatorin transport in rat brain is proton dependent, but oppositely di-

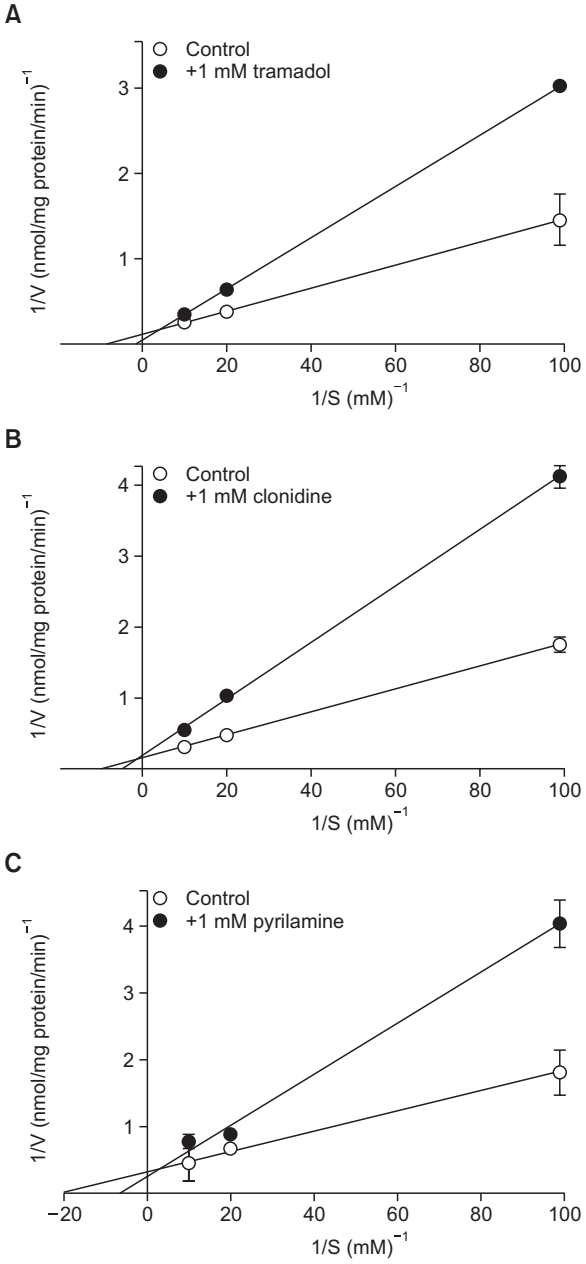


**Fig. 7.** Lineweaver-Burk plots of [$^3$H]imperatorin uptake by TR-BBB cells showing competitive inhibition by tramadol, clonidine and paeonol. [$^3$H]Imperatorin uptake was performed at 37°C for 5 min in the presence (●) or absence (○) of 1 mM tramadol (A), 1 mM clonidine (B) or 1 mM pyrilamine (C). Each point presents the mean ± SEM (n=3).

rected by proton gradient. *In vivo* imperatorin transport into brain was significantly inhibited by various cationic drugs (Table 2). In addition, [$^3$H]imperatorin uptake by rat brain was also markedly inhibited by Pmat and Octn2 substrates. In contract, it was unaffected by ChT, OCTs, Mates, or Octn1 substrates. Moreover, [$^3$H]imperatorin uptake was not inhibited by Oat3 or Mrps substrates (Table 2). BUI experiment was used to confirm this inhibitory result, as result showed imperatorin uptake was significantly inhibited by proton coupled antiporter compound where it was not inhibited by OCTs, Mates, Octn1, Oat3 or Mrps substrates (Table 3). These results support that a carrier-mediated transport process specific for cationic compounds such as Pmat, Octn2 and proton coupled antiporter is possibly involved in the transport of imperatorin to the brain.

Our results also revealed that the initial uptake of [$^3$H]imperatorin by TR-BBB cells was time dependent. It was linearly increased up to 5 min (Fig. 4A). The y-intersection on Fig. 4 was approximately 140 ul/mg protein at 30 sec. This suggests that imperatorin is rapidly adsorbed to cells. *In vitro* uptake of imperatorin was concentration dependent, similar to the *in vivo* result. However, it showed higher affinity and lower capacity than *in vivo* result, with $K_m$ and $V_{max}$ values of 59 μM and 2.22 nmol/(mg protein/min), respectively (Fig. 4B). The saturable component ($V_{max}/K_m$) was estimated to be 37.8 μL/(mg protein×min). This value was 2.2-fold greater than that of nonsaturable uptake clearance $K_d$ at 17 μL/mg protein×min. Its $K_m$ value was also similar to the $K_m$ of cationic drug such as diphenhydramine (59 μM) and tramadol (49 μM) (Kitamura *et al*., 2014) in human blood-brain barrier model (hCMEC/D3 cells) (Sadiq *et al*., 2011). These results provide evidence for the relevance role of carrier-mediated transport for imperatorin uptake into brain.

It is important to identify the function of imperatorin uptake through BBB. Based on *in vitro* cellular uptake study, imperatorin uptake was shown to be sodium- and membrane-potential- independent manner because it was not affected by the replacement of sodium with $NMG^+$, or KCl as well as valinomycin (Table 4). In contrast, it was energy dependent. Moreover, the magnitude of imperatorin uptake at pH 7.4 was significantly higher compared to that at pH 6.4 but lower than that at pH 8.4 (Fig. 5A). Imperatorin uptake by TR-BBB cells was increased after intracellular acidification but decreased after intracellular alkalization (Fig. 5B). It was also significantly inhibited by FCCP, a protonophore (Table 4). Our *in vivo* and *in vitro* results were in agreement with many previous reports showing that the functional transport characteristics of imperatorin through BBB are similar to the characteristics of proton coupled antiporter substrates (Okura *et al*., 2008; André *et al*., 2009; Sadiq *et al*., 2011; Cisternino *et al*., 2013; Shimomura *et al*., 2013). The involvement of proton coupled antiporter in the brain transport of several lipophilic cationic drugs such as pyrilamine, tramadol (Kitamura *et al*, 2014), nicotine (Cisternino *et al*., 2013; Tega *et al*., 2013), diphenhydramine (Cisternino *et al*., 2013), clonidine (Chapy *et al*., 2015) has already been reported in human and mouse BBB as well as in rat BBB. Our *in vivo* and *in vitro* studies also revealed that [$^3$H]imperatorin uptake was markedly inhibited by tramadol, pyrilamine, nicotine, clonidine, and diphenhydramine (Table 2, 5). Especially, [$^3$H]imperatorin uptake was competitively inhibited by tramadol, pyrilamine and clonidine for binding to the transporter with $K_i$ value of 0.19, 0.44 and 1.10 mM, respectively (Fig. 7). *In vivo* and *in vitro* results also showed that imperatorin uptake was inhibited by substances that high lipophilicity (Fig. 8). These data indicated that an influx transporter that related proton coupled antiporter might play a major role in imperatorin transport. However, *in vivo* and *in vitro* results also showed that imperatorin uptake was inhibited by $MPP^+$, ALC and L-carnitine (Table 2, 5). Octn2 has been found in rat brain capillary endothelial cells. It involved in the transport of L-carnitine and acetyl- L-carnitine from the circulating blood to the brain across the BBB. It is mediated by sodium-dependent but pH-

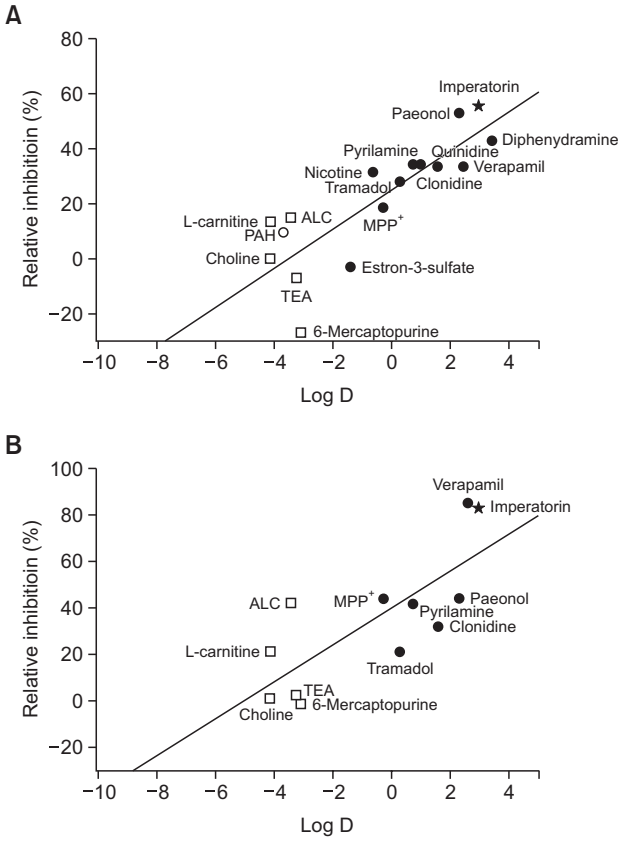


**Fig. 8.** A comparison of the relative inhibitory effect (% of control) and lipophilicity (log D). (A) *In vitro* result of compounds from Table 2. (B) *In vivo* results of compounds from Table 4. Compounds were classified into group I (closed circles, paeonol, primary, secondary and tertiary amines), group II (open square, quaternary amines) and group III (open circles, organic anion drugs). The star represents unlabeled imperatorin.

independent (Kang *et al*., 2002; Miecz *et al*., 2008) Pmat was found to be highly expressed in TR-BBB13 cells and $MPP^+$ was known as a substrate of Pmat. It is energy independence but membrane potential and pH dependent (Okura *et al*., 2011). Thus, they are different from the characteristics of imperatorin uptake by TR-BBB cells identified in this study. In addition, [$^3$H]imperatorin uptake was not reduced in 200 nM of rPmat and rOctn 2 knockdown cells (Fig. 6C). These results suggest that rPmat and rOctn2 do not make significant contribution to imperatorin uptake in TR-BBB cells. Furthermore, our *in vivo* and *in vitro* results showed organic cation such as TEA (classic substrate of sodium- dependent Octs, Octn1 and Mates) had no significant effect on imperatorin uptake by TR-BBB cells and rOct 2 and rOctn1 siRNA transfection did not affect imperatorin uptake (Fig. 6D) (Ohta *et al*., 2006; Hiasa *et al*., 2007). Notably, Octn1 and Mates are known polyspecific organic cation transporters and proton antiporters, both of which are transporters are mediated by membrane potential dependence (Koepsell *et al*, 2007; Terada and Inui, 2008). In addition, [$^3$H]Imperatorin uptake was not significantly inhibited by choline, as classic substrate of sodium-dependent transport system, ChT (Kang *et al*., 2005). There results suggest that Octs, Octn1, Mates, and ChT may not be transport imperatorin in TR-BBB cells.

Lili *et al*. (2013) have demonstrated that imperatorin is not a substrate or inhibitor for the P-glycoprotein (P-gp) because the efflux ratio for imperatorin is 0.5 (if the value is larger than 3.0, it is a substrate of P-gp) and its $IC_{50}$ value is higher than 90 μM. Our studies also suggested that P-gp or organic anion transporter might not play major roles in imperatorin transport at the BBB because [$^3$H]imperatorin uptake into rat brain and by TR-BBB cells were not significantly inhibited by 6-MP, a substrate of Oat3 and Mrps (Table 2, 5) (Deguchi *et al*., 2000; Mori *et al*., 2004; Lee *et al*., 2011). Furthermore, [$^3$H]imperatorin uptake was no significantly affected by with PAH (a substrate of Oat3) (Hosoya *et al*., 2009; Roth *et al*., 2012) and estrone-3-sulfate (a substrate of Oatps) (Sai *et al*., 2006; Roth *et al*., 2012). Especially, our *in vivo* and *in vitro* results showed that [$^3$H]imperatorin uptake was driven by an oppositely directed proton gradient (Fig. 2, 5). Oat3, Oatps and P-gp transport were involved in proton-dependent transport system (Sai *et al*., 2006; Lee *et al*., 2011; Fujii *et al*., 2013).

Based on its neuronal protective effect and its high BBB permeability, imperatorin might be a useful therapeutic candidate for treatment of neurological disorders. It also can be distributed into many regions in rat brain such as cortex, striatum, and hippocampus (Zhang *et al*., 2011). Lee *et al*. (2016) have demonstrated that imperatorin can protect cerebellar granule cells against perfluorohexane sulfonate-induced neuronal apoptosis via inhibiting NMDA receptor/intracellular calcium-mediated ERK pathway, suggesting that imperatorin also ighty be a useful therapeutic candidate for treatment of neurological disorders involving excitotoxicity and neuronal damage. Additional investigation is necessary to characterize the uptake of imperatorin by neurons and astrocytes. Our *in vivo* and *in vitro* experiment was showed same results. Therefore the transport properties of imperatorin are not affected by metabolism or protein binding effect. However, the investigation of it metabolism and protein binding effect is need for the next experiment using high performance liquid chromatography.

Our results demonstrated that the transport mechanism of imperatorin through the BBB involved a proton coupled antiporter. The carrier-mediated system could be responsible for the brain uptake of imperatorin at the BBB which is much more important pharmacokinetically than passive diffusion. These findings suggest that imperatorin might have clinical application as an optimal pharmacotherapy for CNS diseases.

## CONFLICT OF INTEREST

There are no conflict of interest.

## ACKNOWLEDGMENTS

The authors thank Sokheourn Krol for helping *in vivo* experiments. This work was supported by a National Research Foundation of Korea (NRF) grant funded by the Korea government (MSIP) (No. 2011-0030074).

## REFERENCES

Abad, M. J., de las Heras, B., Silván, A. M., Pascual, R., Bermejo, P.,

Rodriquez, B. and Villar, A. M. (2001) Effects of furocoumarins from Cachrys trifida on some macrophage functions. *J. Pharm. Pharmacol.* **53**, 1163-1168.
André, P., Debray, M., Scherrmann, J. M. and Cisternino, S. (2009) Clonidine transport at the mouse blood-brain barrier by a new H+ antiporter that interacts with addictive drugs. *J. Cereb. Blood Flow Metab.* **29**, 1293-1304.
Baek, N. I., Ahn, E. M., Kim, H. Y. and Park, Y. D. (2000) Furanocoumarins from the root of Angelica dahurica. *Arch. Pharm. Res.* **23**, 467-470.
Budzynska, B., Boguszewska-Czubara, A., Kruk-Slomka, M., Skalicka-Wozniak, K., Michalak, A., Musik, I. and Biala, G. (2015) Effects of imperatorin on scopolamine-induced cognitive impairment and oxidative stress in mice. *Psychopharmacology (Berl.)* **232**, 931-942.
Budzynska, B., Kruk-Slomka, M., Skalicka-Wozniak, K., Biala, G. and Glowniak, K. (2012) The effects of imperatorin on anxiety and memory-related behavior in male Swiss mice. *Exp. Clin. Psychopharmacol.* **20**, 325-332.
Chapy, H., Smirnova, M., André, P., Schlatter, J., Chiadmi, F., Couraud, P. O., Scherrmann, J. M., Declèves, X. and Cisternino, S. (2014) Carrier-mediated cocaine transport at the blood-brain barrier as a putative mechanism in addiction liability. *Int. J. Neuropsychopharmacol.* **18**, pyu001.
Chapy, H., Goracci, L., Vayer, P., Parmentier, Y., Carrupt, P. A., Declèves, X., Scherrmann, J. M., Cisternino, S. and Cruciani, G. (2015) Pharmacophore-based discovery of inhibitors of a novel drug/proton antiporter in human brain endothelial hCMEC/D3 cell line. *Br. J. Pharmacol.* **172**, 4888-4904.
Cisternino, S., Chapy, H., André, P., Smirnova, M., Debray, M. and Scherrmann, J. M. (2013) Coexistence of passive and proton antiporter-mediated processes in nicotine transport at the mouse blood-brain barrier. *AAPS J.* **15**, 299-307.
Deguchi, Y., Yokoyama, Y., Sakamoto, T., Hayashi, H., Naito, T., Yamada, S. and Kimura, R. (2000) Brain distribution of 6-mercaptopurine is regulated by the efflux transport system in the blood-brain barrier. *Life.Sci.* **66**, 649-662.
Fujii, S., Hayashi, H., Itoh, K., Yamada, S., Deguchi, Y. and Kawazu, K. (2013) Characterization of the carrier-mediated transport of ketoprofen, a nonsteroidal anti-inflammatory drug, in rabbit corneal epithelium cells. *J. Pharm. Pharmacol.* **65**, 171-180.
Hosoya, K., Makihara, A., Tsujikawa, Y., Yoneyama, D., Mori, S., Terasaki, T., Akanuma, S., Tomi, M. and Tachikawa, M. (2009) Roles of inner blood-retinal barrier organic anion transporter 3 in the vitreous/retina-to-blood efflux transport of p-aminohippuric acid, benzylpenicillin, and 6-mercaptopurine. *J. Pharmacol. Exp. Ther.* **329**, 87-93.
Hiasa, M., Matsumoto, T., Komatsu, T., Omote H. and Moriyama, Y. (2007) Functional characterization of testis-specific rodent multidrug and toxic compound extrusion 2, a class III MATE-type polyspecific $H^+$/organic cation exporter. *Am. J. Physiol., Cell Physiol.* **293**, C1437-C1444.
Kang, Y. S., Lee, K. E., Lee, N. Y. and Terasaki, T. (2005) Donepezil, tacrine and alpha-phenyl-n-tert-butyl nitrone (PBN) inhibit choline transport by conditionally immortalized rat brain capillary endothelial cell lines (TR-BBB). *Arch. Pharm. Res.* **28**, 443-450.
Kang, Y. S., Ohtsuki, S., Takanaga, H., Tomi, M., Hosoya, K. and Terasaki, T. (2002) Regulation of taurine transport at the blood-brain barrier by tumor necrosis factor-alpha, taurine and hypertonicity. *J. Neurochem.* **83**, 1188-1195.
Kang, Y. S. (2000) Taurine transport mechanism through the blood-brain barrier in spontaneously hypertensive rats. *Adv. Exp. Med. Biol.* **483**, 321-324.
Kido, Y., Tamai, I., Ohnari, A., Sai, Y., Kagami, T., Nezu, J., Nikaido, H., Hashimoto, N., Asano, M. and Tsuji, A. (2001) Functional relevance of carnitine transporter OCTN2 to brain distribution of L-carnitine and acetyl-L-carnitine across the blood-brain barrier. *J. Neurochem.* **79**, 959-969.
Kim, D. K., Lim, J. P., Yang, J. H., Eom, D. O., Eun, J. S. and Leem, K. H. (2002) Acetylcholinesterase inhibitors from the roots of Angelica dahurica. *Arch. Pharm. Res.* **25**, 856-859.
Kitamura, A., Higuchi, K., Okura, T. and Deguchi, Y. (2014) Transport characteristics of tramadol in the blood-brain barrier. *J. Pharm. Sci.* **103**, 3335-3341.
Koepsell, H., Lips, K. and Volk C. (2007) Polyspecific organic cation transporters: structure, function, physiological roles, and biopharmaceutical implications. *Pharm. Res.* **24**, 1227-1251.
Kozioł, E. and Skalicka-Woźniak, K. (2016) Imperatorin-pharmacological meaning and analytical clues: profound investigation. *Phytochem. Rev.* **15**, 627-649.
Kubo, Y., Kusagawa, Y., Tachikawa, M., Akanuma, S. and Hosoya, K. (2013) Involvement of a novel organic cation transporter in verapamil transport across the inner blood-retinal barrier. *Pharm. Res.* **30**, 847-856.
Lee, E., Choi, S. Y., Yang, J. H. and Lee, Y. J. (2016) Preventive effects of imperatorin on perfluorohexanesulfonate-induced neuronal apoptosis via inhibition of intracellular calcium-mediated ERK pathway. *Korean J. Physiol. Pharmacol.* **20**, 399-406.
Lee, N. Y., Lee, K. B. and Kang, Y. S. (2014) Pharmacokinetics, placenta, and brain uptake of paclitaxel in pregnant rats. *Cancer Chemother. Pharmacol.* **73**, 1041-1045.
Lee, N. Y. and Kang, Y. S. (2016) *In vivo* and *in vitro* evidence for brain uptake of 4-Phenylbutyrate by the monocarboxylate transporter 1 (MCT1). *Pharm. Res.* **33**, 1711-1722.
Lee, N. Y., Sai, Y., Nakashima, E., Ohtsuki, S. and Kang, Y. S. (2011) 6-Mercaptopurine transport by equilibrative nucleoside transporters in conditionally immortalized rat syncytiotrophoblast cell lines TR-TBTs. *J. Pharm. Sci.* **100**, 3773-3782.
Lili, W., Yehong, S., Qi, Y., Yan, H., Jinhui, Z., Yan, L. and Cheng, G. (2013) *In vitro* permeability analysis, pharmacokinetic and brain distribution study in mice of imperatorin, isoimperatorin and cnidilin in Radix Angelicae Dahuricae. *Fitoterapia* **85**, 144-153.
Miecz, D., Januszewicz, E., Czeredys, M., Hinton, B. T., Berezowski, V., Cecchelli, R. and Nałecz, K. A. (2008) Localization of organic cation/carnitine transporter (OCTN2) in cells forming the blood-brain barrier. *J. Neurochem.* **104**, 113-123.
Mori, S., Ohtsuki, S., Takanaga, H., Kikkawa, T., Kang, Y. S. and Terasaki, T. (2004) Organic anion transporter 3 is involved in the brain-to-blood efflux transport of thiopurine nucleobase analogs. *J. Neurochem.* **90**, 931-941.
Ohta, K. Y., Inoue, K., Hayashi, Y. and Yuasa, H. (2006) Molecular identification and functional characterization of rat multidrug and toxin extrusion type transporter 1 as an organic cation/H+ antiporter in the kidney. *Drug Metab. Dispos.* **34**, 1868-1874.
Ohtsuki, S. and Terasaki, T. (2007) Contribution of carrier-mediated transport systems to the blood-brain barrier as a supporting and protecting interface for the brain; importance for CNS drug discovery and development. *Pharm. Res.* **24**, 1745-1758.
Okura, T., Hattori, A., Takano, Y., Sato, T., Hammarlund-Udenaes, M., Terasaki, T. and Deguchi, Y. (2008) Involvement of the pyrilamine transporter, a putative organic cation transporter, in blood-brain barrier transport of oxycodone. *Drug Metab. Dispos.* **36**, 2005-2013.
Okura, T., Kato, S., Takano, Y., Sato, T., Yamashita, A., Morimoto, R., Ohtsuki, S., Terasaki, T. and Deguchi, Y. (2011) Functional characterization of rat plasma membrane monoamine transporter in the blood-brain and blood-cerebrospinal fluid barriers. *J. Pharm. Sci.* **100**, 3924-3938.
Pardridge, W. M., Kang, Y. S. and Buciak, J. (1994) Transport of human recombinant brain-derived neurotrophic factor (BDNF) through the rat blood-brain barrier *in vivo* using vector-mediated peptide drug delivery. *Pharm. Res.* **11**, 738-746.
Roth, M., Obaidat, A. and Hagenbuch, B. (2012) OATPs, OATs and OCTs: the organic anion and cation transporters of the *SLCO* and *SLC22A* gene superfamilies. *Br. J. Pharmacol.* **165**, 1260-1287.
Sadiq, M. W., Borgs, A., Okura, T., Shimomura, K., Kato, S., Deguchi, Y., Jansson, B., Björkman, S., Terasaki, T. and Hammarlund-Udenaes, M. (2011) Diphenhydramine active uptake at the blood-brain barrier and its interaction with oxycodone *in vitro* and *in vivo*. *J. Pharm. Sci.* **100**, 3912-3923.
Sai, Y., Kaneko, Y., Ito, S., Mitsuoka, K., Kato, Y., Tamai, I., Artursson, P. and Tsuji, A. (2006) Predominant contribution of organic anion transporting polypeptide OATP-B (OATP2B1) to apical uptake of estrone-3-sulfate by human intestinal Caco-2 cells. *Drug Metab.*

*Dispos.* **34**, 1423-1431.

Sancho, R., Márquez, N., Gómez-Gonzalo, M., Calzado, M. A., Bettoni, G., Coiras, M. T., Alcamí, J., López-Cabrera, M., Appendino, G. and Muñoz, E. (2004) Imperatorin inhibits HIV-1 replication through an Sp1-dependent pathway. *J. Biol. Chem.* **279**, 37349-37359.

Senol, F. S., Woźniak, K. S., Khan, M. T. H., Orhan, I. E., Sener, B. and Głowniak, K. (2011) An *in vitro* and *in silico* approach to cholinesterase inhibitory and antioxidant effects of the methanol extract, furanocoumarin fraction, and major coumarins of Angelica officinalis L. fruits. *Phytochem. Lett.* **4**, 462-467.

Shimomura, K., Okura, T., Kato, S., Couraud, P. O., Schermann, J. M., Terasaki, T. and Deguchi, Y. (2013) Functional expression of a proton-coupled organic cation (H+/OC) antiporter in human brain capillary endothelial cell line hCMEC/D3, a human blood-brain barrier model. *Fluids Barriers CNS* **10**, 8.

Sigurdsson, S. and Gudbjarnason, S. (2007) Inhibition of acetylcholinesterase by extracts and constituents from Angelica archangelica and Geranium sylvaticum. *Z. Naturforsch., C, J. Biosci.* **62**, 689-693.

Stavri, M. and Gibbons, S. (2005) The antimycobacterial constituents of dill (Anethum graveolens). *Phytother. Res.* **19**, 938-941.

Suzuki, T., Moriki, Y., Goto, H., Tomono, K., Hanano, M. and Watanabe, J. (2002) Investigation on the influx transport mechanism of pentazocine at the blood-brain barrier in rats using the carotid injection technique. *Biol. Pharm. Bull.* **25**, 1351-1355.

Takasato, Y., Rapoport, S. I. and Smith, Q. R. (1984) An *in situ* brain perfusion technique to study cerebrovascular transport in the rat. *Am. J. Physiol.* **247**, H484-H493.

Tamai, I., Nakanishi, T., Kobayashi, D., China, K., Kosugi, Y., Nezu, J., Sai, Y. and Tsuji, A. (2004) Involvement of OCTN1 (SLC22A4) in pH-dependent transport of organic cations. *Mol. Pharm.* **1**, 57-66.

Tega, Y., Akanuma, S., Kubo, Y., Terasaki, T. and Hosoya, K. (2013) Blood-to-brain influx transport of nicotine at the rat blood-brain barrier: involvement of a pyrilamine-sensitive organic cation transport process. *Neurochem. Int.* **62**, 173- 181.

Terada, T. and Inui, K. (2008) Physiological and pharmacokinetic roles of H+/organic cation antiporters (MATE/SLC47A). *Biochem. Pharmacol*. **75**, 1689-1696.

Terasaki, T. and Hosoya, K. (2001) Conditionally immortalized cell lines as a new *in vitro* model for the study of barrier functions. *Biol. Pharm. Bull.* **24**, 111-118.

Wu, D., Kang, Y. S., Bickel, U. and Pardridge, W. M. (1997) Blood-brain barrier permeability to morphine-6-glucuronide is markedly reduced compared with morphine. *Drug Metab. Dispos.* **25**, 768-771.

Wu, D. and Pardridge, W. M. (1999) Blood-brain barrier transport of reduced folic acid. *Pharm. Res*. **16**, 415-419.

Zhang, X., Xie, Y., Cao, W., Qian, Y., Shan, M. and Siwang, W. (2011) Brain distribution study of imperatorin in rats after oral administration assessed by HPLC. *Chromatographia* **74**, 259-265.